Journal of Porous Materials (2021) 28:1439–1448
https://doi.org/10.1007/s10934-021-01098-w

Identification of active structure and catalytic efficiency of MCM-22 zeolite detemplated by two different processes

Abbas Al-Nayili[1] · **Mushtaq Albdiry**[2,3]

Accepted: 28 May 2021 / Published online: 31 May 2021

Abstract
This study attempts to identify the active structure and the catalytic efficiency of MCM-22 zeolite after the successful removal of pre-synthesized MCM-22(P) template by two different methods. The MCM-22(P) zeolite was firstly synthesized by hydrothermal process with a SiO_2/Al_2O_3 ratio of 50, and its 2D layered hexamethyleneimine (HMI) precursor template was removed by (i) thermal calcination at high temperature (550 °C) to obtain the MCM-22(C), and (ii) oxidation with H_2O_2 treatment at low temperature (90 °C) to obtain the MCM-22(H_2O_2). The structural characteristics of MCM-22(C) and the MCM-22(H_2O_2) were identified by XRD, N_2 absorption/desorption, FTIR, NH_3-TPD and ^{27}Al MAS-NMR. The catalytic performance of MCM-22(C) and MCM-22(H_2O_2) loaded by 20 wt% zinc nanoparticles were examined through a Friedel-Grafts (FC) alkylation of benzene with benzyl chloride in a liquid phase environment. It was found that Zn-MCM-22(H_2O_2) was more efficient in FC alkylation reaction in comparison with Zn-MCM-22(C) for the formation of intercrystal pores due to the inhibitory influence of silonal group condensation on the external surface of MCM-22 crystals.

Keywords MCM-22 zeolite · Detemplation · H_2O_2 · Friedel–Crafts alkylation · Thermal calcination

1 Introduction

The MCM-22 zeolite has a unique crystal structure with an arrangement consisting of two different pore structures. One is made up of two-dimensional sinusoidal channels with 10MR pore openings, and the other is 12MR interlayer supercages [1]. This unique structure of the MCM-22 zeolite enables it to be used as an efficient catalyst for different chemical catalytic reactions such as cracking [2], disproportionation [3], esterification [4] and isomerization [5]. To synthesize the MCM-22 zeolite, the precursor MCM-22(P) was prepared first, and having a 2D layered structure of MWW layers interact together via hydrogen bonds in the neighbouring surfaces between silanol (Si–OH) groups [6, 7]. Second, this structured directing agent (or template) has to be removed by the thermal calcination which resulted in condensing silanol groups and forming corresponding 3-dimensional MCM-22 zeolite [8]. The thermal calcination is a commonly conducted process for the removal of template from zeolite structures, but it has several disadvantages where it may cause the distortion of thin layers of the MWW type, and distortion of a part of 10-ring channels and 12-ring pockets [9]. The higher temperatures required to complete the thermal calcination may also cause a further condensation of silanol groups, that is in turn affecting the intercrystal porosity, crystal agglomeration and a reduction in the overall surface area [10, 11]. Another side effect of high temperature calcination is the extraction of frame aluminum and partial amorphization due to high local temperatures during the calcination process [12]. Thus, the template's removal of MCM-22 via the thermal calcination would not be a perfect method to produce a good catalytic efficiency. Hence, other template removal techniques such as hydrocracking [13], microwave irradiation [14], and oxidative gases (e.g., NO_2 and N_2O) [15] were developed to extract the template from the zeolites. These techniques, however, require relatively

✉ Abbas Al-Nayili
abbas.al-nayili@qu.edu.iq

✉ Mushtaq Albdiry
mushtaq.albdiry@curtin.edu.au

[1] Department of Chemistry, University of Al-Qadisiyah, Al Diwaniyah City, Iraq

[2] Department of Materials Engineering, University of Al-Qadisiyah, Al Diwaniyah City, Iraq

[3] Department of Mechanical Engineering, School of Civil and Mechanical Engineering, Curtin University, GPO Box U1987, Perth City, WA 6845, Australia

high temperatures (> 200 °C) for successfully removing of the template. To overcome this concern, Xing et al. [16] have recently attempted a mild detemplation approach of handling MCM-56 zeolite by a direct treatment with H_2O_2 at low temperatures. Similaly, a novel ITQ-2-like zeolite was successfully synthesized by treating the MCM-22 precursor with H_2O_2 [17]. Moreover, BEA zeolite was detemplated by treating with a Fenton's-type reagent (Fe^{3+}–H_2O_2) [18]. Nevertheless, there is a lack in research addressing the detemplation process of the zeolites particularly in the oxidation of MCM-22 with H_2O_2 solution. Importantly, the role of using different techniques namely thermal calcination and H_2O_2 oxidation in removing MCM-22 zeolites' templates on their catalytic activities in the conversion of benzene alkylation through Friedel Crafts reaction has not been addressed well. Also, the role of supporting detemplated MCM-22 zeolites by zinc nanoparticles on their acidity sites and thereof the activity through Friedel Crafts reaction has not thoroughly considered except [19] a conducted reaction to convert benzene through Zn-MCM-22 catalyst.

In the present study, a comprehensive comparison between the effects of the extraction process of MCM-22 template using the thermal calcination at high temperatures and the extraction by direct treatment with H_2O_2 at a low temperature was conducted. The obtained active structure of the MCM-22 detemplated by both methods was identified by XRD, SEM, N_2 adsorption/desorption, FTIR, ^{27}Al MAS NMR spectra, and the NH_3-TPD profiles. The catalytic activity of the detemplated MCM-22 zeolites by both methods after its being loaded with 20 wt% Zn metal was evaluated via the alkylation process of benzene with benzyl chloride in liquid phase through a Friedel–Crafts alkylation reaction.

2 Experimental part

2.1 Preparation of the MCM-22(P)

The MCM-22(P) precursor zeolite, which has a SiO_2/Al_2O_3 ratio of 50, was hydrothermally synthesized following the procedure described by Corma et al. [20]. A fumed silica (SiO_2, Cab-o-Sil M5) was used as a Si source, $NaAlO_2$ (33% Al_2O_3, 35.5% Na_2O, Aldrich) as Al source, NaOH (99.5%, Merck) and hexamethyleneimine (HMI, 99%, Aldrich) as a template material. The mixed gel was put inside a PTFE-lined stainless-steel autoclave, stirred at 60 rpm and heated at 150 °C for 10 days. The product was thoroughly washed with deionized water and dried in an oven at 60 °C overnight.

2.2 Removal of the HMI template

In this study, two detemplation methods were applied to remove the organic template (HMI) from the synthesized MCM-22(P). The first is the MCM-22(P) was detemplated by using the thermal calcination, inside a vacuum tube furnace at 550 °C for 5 h to obtain the MCM-22(C). The other is the MCM-22(P) which was oxidized twice with 30% H_2O_2 solution (liquid/solid ratio = 5 cm^3/g) in a flask under continuous stirring at 90 °C for 20 h to obtain the MCM-22(H_2O_2).

2.3 Synthesis of the catalysts

After the preparation of MCM-22(P) zeolites and their templates removal, the obtained MCM-22(C) and the MCM-22(H_2O_2) catalysts were loaded by 20 wt% Zn, zinc nanoparticles. An incipient impregnation technique was used to deposit the Zn metal from zinc chloride ($ZnCl_2$, 99.0%, Aldrich) as a precursor. A 2 g $ZnCl_2$ powder was dissolved in 50 ml methanol, and added into a 10 g MCM-22(C) and another 10 g MCM-22(H_2O_2) precursor at a continuous stirring in a small aliquots with 1 ml/min. The resultant paste was dried for 3 h at 120 °C to remove any remaining water and occluded volatiles before being calcined at 200 °C following a 2 °C/min as a ramp rate**.** To better undertand the synthesis process and two detemplation process of the MCM-22 used in the study, a schematic sketch is provided in Fig. 1.

2.4 Characteristics of the catalysts

The XRD analysis of the synthesized zeolites was conducted by Siemens D-5000 with Cu-kα radiation in the range of 5–55° (2θ) at 40 kV and 30 mA. The morphological characteristics of MCM-22(H_2O_2) and MCM-22(C) were examined using SEM-JSM-6010 LV. The N_2 adsorption/desorption analysis was determined by a Micromeritics ASAP 2000 to identify the role of two detemplation methods on the physicochemical properties of MCM-22(C) and MCM-22(H_2O_2) zeolites. The FTIR analysis and ^{27}Al MAS NMR spectrometer of all zeolites were measured by Bruker Vector-22 and Varian VXR-400S, respectively. The acidic nature of the catalyst was analyzed with Chemisorb 275050 by temperature-programmed ammonia desorption (NH_3-TPD). A Microwave Plasma Atomic Emission Spectroscopy (model 4100-MP-AES) was used to examine the probability of Zn leaching from the catalyst, and analyze the filtrated solutions after the reaction.

2.5 Evaluation of catalytic efficiency

20 wt% Zn-MCM-22(C) and Zn-MCM-22(H_2O_2) catalysts were prepared and tested for the benzylation of benzene with BC to investigate the effectivencess of these two detemplation methods. 0.025 mol BC and 0.5 mol benzene (mole BC/mole benzene = 20) were prepared as a standard benzylation solution with a catalyst load of 25 mg cm^{-3}. Samples were

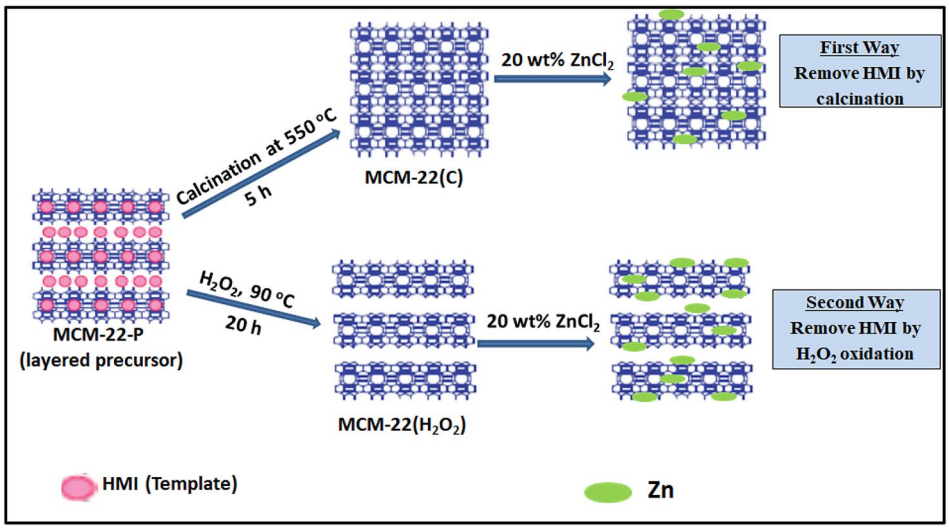

Fig. 1 A schematic describtion of the synthesis process and two detmeplation methods of the MCM-22 used in this study

collected and analyzed by using a gas chromatograph (HP-6890) fortified with a capillary column and FID detector.

3 Results and discussion

3.1 XRD and SEM analysis

Figure 2A displays the XRD patterns of the prepared precursor MCM-22(P), and the detemplated samples of MCM-22(C) and MCM-22(H_2O_2) zeolites. The MCM-22(P) XRD pattern is in line with those presented in literature [19, 21]. Moreover, at 2θ values of 7.1 and 7.8, two diffraction peaks at (101) and (102) suggest the organized layered arrangement of MCM-22(P) along with the perpendicularly aligned layers arranged vertically to the c axis [22]. Prior to template removal, the diffraction peaks in the 2 range of 13–30° are wide, and some of them overlap. Thermal calcination and H_2O_2 treatment all resulted in major improvements in the XRD patterns of MCM-22(P) after the template was removed. The diffraction peak of (002) plane at 2θ = 6.6° for MCM-22(P) indicates the MWW stacking layers. This peak, however, had disappeared in the XRD patterns of MCM-22(C) and MCM-22(H_2O_2). A reflection peak at 2θ = 7.1° band for the (100) plane corresponding to the MWW intra-layer can be observed in XRD patterns of all MCM-22 zeolites. The intensity of this peak is much higher in the XRD pattern for the H_2O_2 treated zeolite than that for the calcined one. This indicates that the template elimination by H_2O_2 treatment can attenuate the collapse of the

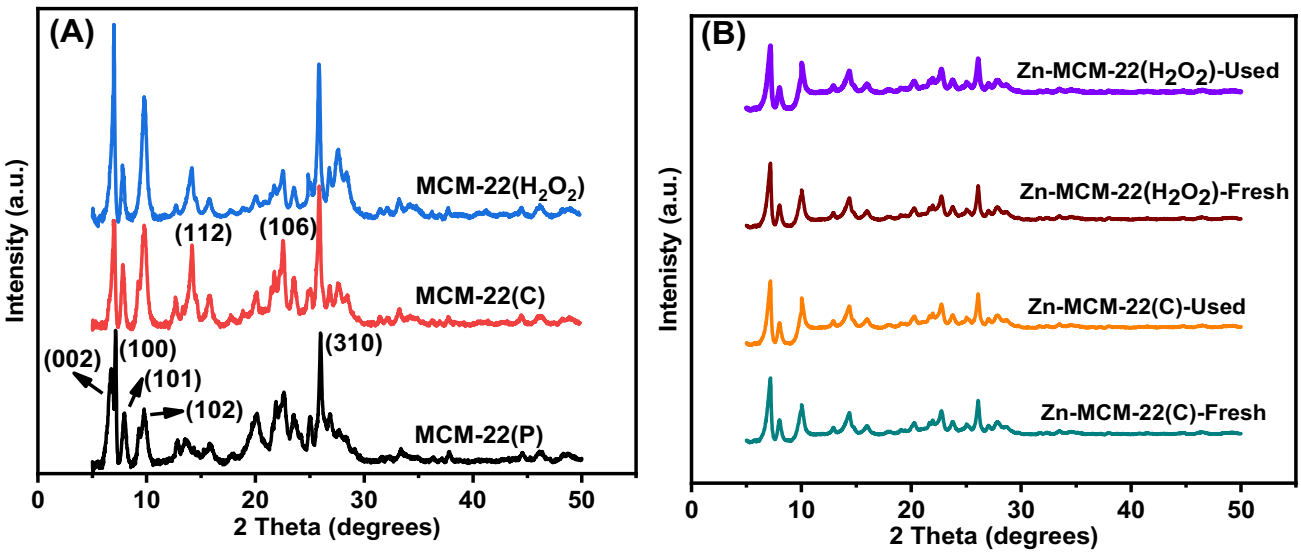

Fig. 2 XRD powder patterns for the **A** MCM-22 samples and **B** fresh and used Zn-MCM-22 catalysts

zeolite structure which was also evidenced by the results of ^{27}AL MAS NMR (Fig. 7). This could be attributed to the reduction of dealumination because of the lower temperature of H_2O_2 treatment. In additions, the XRD patterns of both MCM-22(C) and MCM-22(H_2O_2) had a number of broad intensities at $2\theta = 12.5°$ for (112) plane and 23.3° for (106) plane indicating the condensation of the terminal silanol groups (–Si–O–H) on the MCM-22(C) sheets [23]. Interestingly, these intensities seem to be shorter in the MCM-22(H_2O_2) for the lower condensation of the terminal silanol groups verified by the results of textural properties of MCM-22(H_2O_2). The peak at wide angles of $2\theta = 26.2°$ band corresponding for the (310) plane appeared in all the XRD patterns, and this means that the template removal from the MCM-22(P) structure did not affect the crystallinity of the MCM-22 regardless of the type of the removal method whether thermal calcination or H_2O_2 oxidation. Figure 2B shows the differences in XRD patterns between the Zn-MCM-22(C), Zn-MCM-22(H_2O_2) and those of MCM-22(C), MCM-22(H_2O_2) which are mostly due to the relative intensity of the (100) and (101) XRD peaks. For MCM-22(C) and Zn-MCM-22(C), the ratio falls from 1.62 to 1.41, while in the MCM-22(H_2O_2) and Zn-MCM-22(H_2O_2) falls from 1.88 to 1.31. This difference in the XRD intensity suggesting that Zn atoms are incorporated in the framework of MCM-22. The XRD peaks of the Zn-MCM-22(C) and Zn-MCM-22(H_2O_2) appear after being used in the conversion reaction. There is no significant difference can be noted from the intensity of the diffraction peaks of the fresh and used catalysts, indicating the stability of these catalysts even after use.

The morphological characteristics of the fresh MCM-22(H_2O_2) and fresh MCM-22(C) catalysts were examined using SEM analysis as shown in Fig. 3A and B. We can clearly observe a dense, bright and more porous structure of the MCM-22(H_2O_2) versus a coarser and rougher structure of the MCM-22(C).

The EDX analysis as described in Table 1, was used to determine the weight percentages of Zn particles loaded on the fresh and used MCM-22(C) and MCM-22(H_2O_2) catalysts.

3.2 N_2 adsorption/desorption analysis

The MCM-22(C) and MCM-22(H_2O_2) zeolites' N_2 adsorption/desorption isotherms are depicted in Fig. 4. In general, the MCM-22 zeolite depicts type I isotherm for its microporous structure [24]. From this figure, it can be obviously seen that the hysteresis loop of the MCM-22(H_2O_2) is a little wider and higher than the loop of the calcined MCM-22. This could be attributed to the increment of the surface area and increment in the mesoporous structure of the zeolite detemplated by H_2O_2 treatment.

Table 2 lists the textural properties including the surface area and the pore volume for the detemplated zeolites. The total surface area of the zeolite detemplated by H_2O_2 treatment (605.18 $cm^2\ g^{-1}$) seems to be larger than that for the zeolite detemplated by thermal calcination (513.22 $cm^2\ g^{-1}$)

Table 1 EDX analysis of the fresh and used catalysts

Catalyst	Zn loading EDX (wt%)	
	Fresh	Used
Zn-MCM-22(C)	20.1	(19.99)[a](20.1)[b]
Zn-MCM-22(H_2O_2)	20	(20.05)[a](19.98)[b]

[a]1st used

[b]5th used

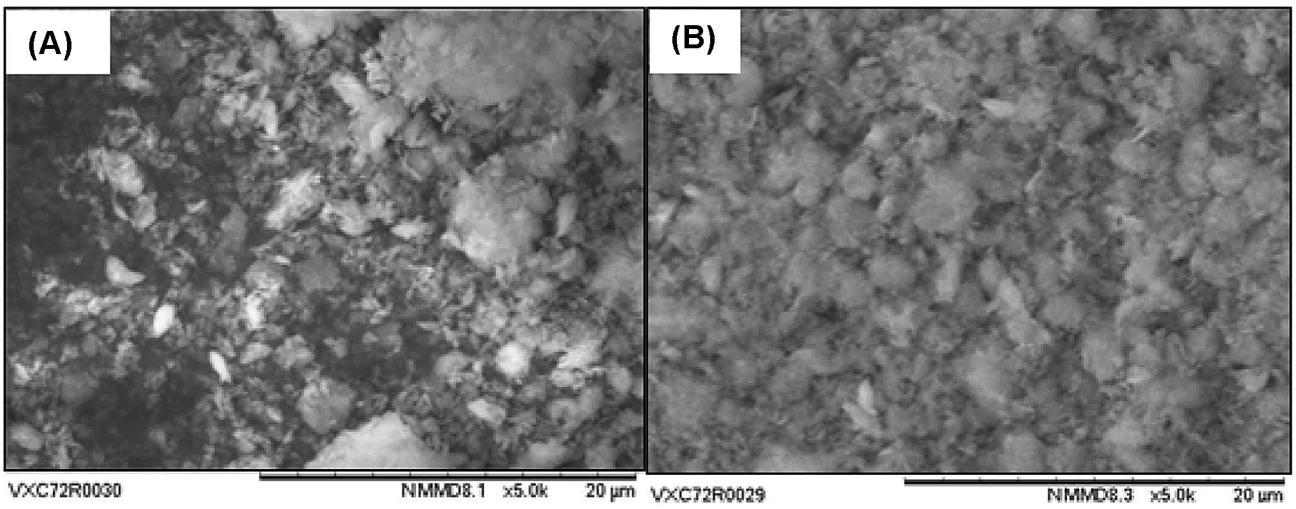

Fig. 3 SEM images of **A** fresh MCM-22(H_2O_2) and **B** fresh MCM-22(C)

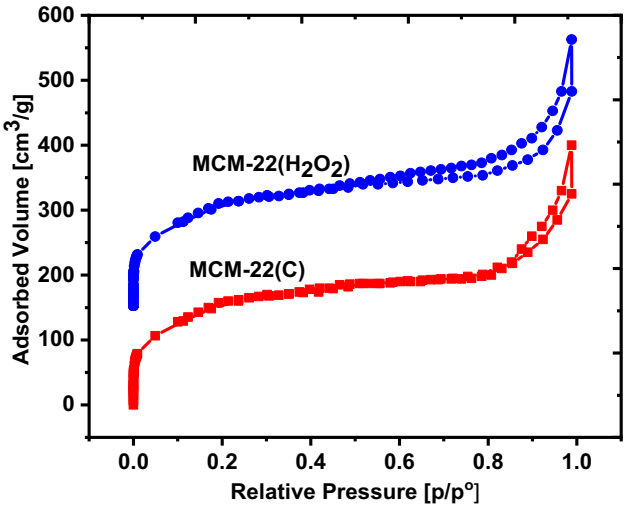

Fig. 4 N_2 adsorption/desorption isotherms of the MCM-22(C) and MCM-22(H_2O_2)

by almost 18% increase. Similarly, the exterior surface area and the pore volume of the MCM-22(H_2O_2) zeolite were bigger by 33% and 11.5%, respectively than those values of the MCM-22(C) zeolite.

The increased surface area and the pore volume due to the template removed from the MCM-22(P) by H_2O_2 treatment induced a lesser condensation of the Si–OH silanol groups connected to the MWW layer by hydrogen bonding, and it also induced the formation of inter and intra-crystal mesopores [11]. Table 2 shows that the H_2O_2 treatment exposed more 10-ring channels and 12-ring pockets in the synthesized zeolite, resulting in increased microporous surface area (S_{micro}) and microporous volume (V_{micro}) of the MCM-22(H_2O_2). In terms of the calcined zeolites, the heat produced during the direct thermal calcination will cause more structural agglomeration and distortion of zeolite particles, ending with the creation of some piled pores [16].

3.3 FTIR analysis

The FT-IR spectra of the MCM-22(P), MCM-22(C) and MCM-22(H_2O_2) zeolites have been illustrated by Fig. 5. The FTIR spectrum for the MCM-22(P) zeolite exhibited band at 1455 cm^{-1} is attributed to –NH– groups. Moreover, the bands at 1469 cm^{-1} (C–H bending vibrations), 2863 cm^{-1} and 2935 cm^{-1} (C–H stretching vibration) of the template can be easily observed. This finding was in conformance with [25]. These bands, however disappeared in the FTIR spectra of the MCM-22-C and the MCM-22-H_2O_2 zeolite. This indicates that the molecules template was successfully removed by thermal calcination and H_2O_2 oxidation and showed a similar effect on the vibrational relaxation and chemical bonding structure.

Figure 6 depicts the TGA-DTA spectra for the precursor MCM-22(P), detemplated MCM-22(C) and MCM-22(H_2O_2), and Zn-MCM-22(C) and Zn-MCM-22(H_2O_2)

Table 2 Textural properties of the MCM-22(C) and MCM-22(H_2O_2)

Materials	S_{Total} (m^2 g^{-1})	S_{micro} (m^2 g^{-1})	S_{exter} (m^2 g^{-1})	V_{micro} (cm^3 g^{-1})
MCM-22(C)	513.22	358.14	155.08	0.191
MCM-22(H_2O_2)	605.18	399.06	206.12	0.213

T-plot approach is approved for total surface area and microporous area and pore volume

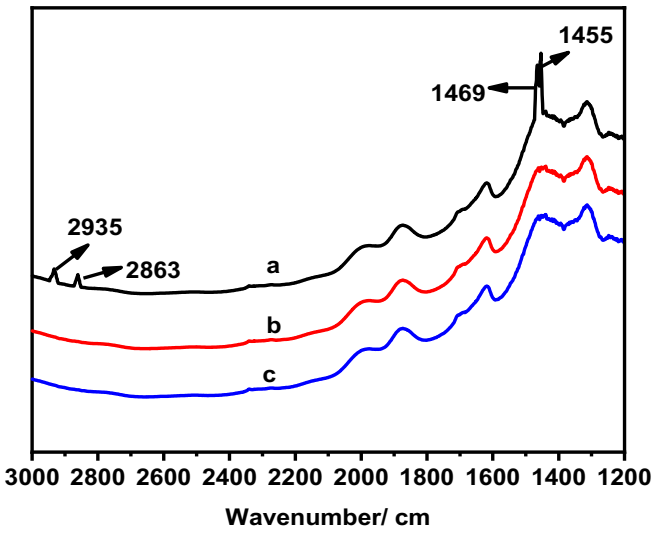

Fig. 5 FT-IR spectra of the zeolite frameworks: (a) MCM-22(P), (b) MCM-22(C) and (c) MCM-22(H_2O_2)

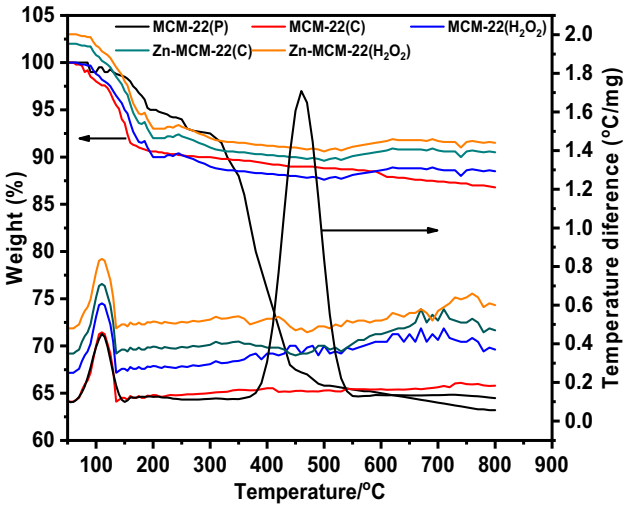

Fig. 6 The TGA-DTA curves of the synthesized catalysts

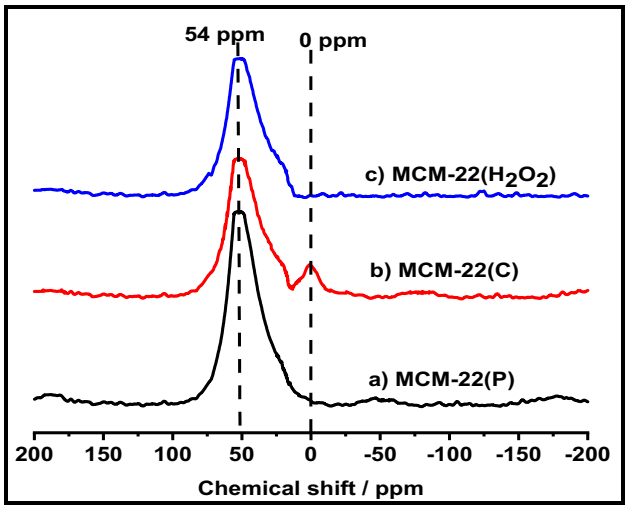

Fig. 7 The ^{27}Al MAS NMR spectra for the MCM-22(P) (a), MCM-22(C) (b) and MCM-22(H_2O_2) (c)

zeolites. The weight loss from MCM-22(P) was 32%, while it was 1.35% and 1.81% for the MCM-22(C) and MCM-22(H_2O_2) in the temperature range of 120–600 °C, respectively. The DTA profile of the MCM-22(P) had two large weight losses, the first was around 100 °C caused by physisorbed water and the other of 400–550 °C for the template. The DTA profle of the MCM-22(C), MCM-22(H_2O_2), Zn-MCM-22(C) and Zn-MCM-22(H_2O_2) revealed an apparent weight loss around 100 °C for the physisorbed water while the other peak disappeared due to the template removal.

3.4 The ^{27}Al-MAS NMR analysis

The ^{27}Al-MAS NMR spectroscopy is used to investigate the coordination environment of the Al atoms in the zeolitic structures. Figure 7 displays the ^{27}Al MAS NMR spectra for the synthesized MCM-22(P), MCM-22(C) and MCM-22(H_2O_2). The ^{27}Al-MAS NMR spectrum (Fig. 7a) of the precursor MCM-22(P) zeolite with the organic template (HMI) has only one peak at 54 ppm resonance band referring to a tetrahedrally coordinated Al [26]. In Fig. 7b, two peaks can be observed, the first lies at about 54 ppm indicating the existing tetrahedrally coordinated Al framework. The other peak lies at about 0 ppm indicating the existence of Al as an octahedrally coordinated extra-framework [27, 28], which showed that thermal calcination can significantly enhance MCM-22 dealumination. However, in terms of using H_2O_2-oxidation (Fig. 7c) for the template removal, it seems that there is no extra-frame Al species present (0 ppm), and all aluminium stays tetrahedrally coordinated (54 ppm). It can be concluded that H_2O_2 treatment has efficiently reduced the dealumination process of the MCM-22, and inhibited the condensation of the Si–OH silanol groups on the surface of the MCM-22 crystals due to the reduced temperature treatment.

3.5 The NH_3-TPD analysis

The NH_3-TPD desorption analysis was used to measure the surface concentration of acid sites and their intensity distribution, and the findings are presented in Fig. 8. Both MCM-22(C) and MCM-22(H_2O_2) have two NH_3 desorption peaks, which relate to the weak as well as strong acidic sites [22]. For the MCM-22(C), the temperature of the initial NH_3-desorption peak is around 190 °C that is lower than 202 °C for the MCM-22(H_2O_2). The temperature of the next NH_3-desorption peak; however, is very close to 374 °C for both MCM-22(C) and MCM-22(H_2O_2). These findings showed that the acid concentration of the weak acidic sites of MCM-22(H_2O_2) is higher than those of MCM-22(C), whereas the acid concentration of the strong acidic sites of MCM-22(C) and MCM-22(H_2O_2) proves to be almost identical. The overall number of acidic sites over MCM-22(H_2O_2) is obviously greater than MCM-22(C) due to the greater concentration of bridging hydroxyl groups (SiOHAl) of MCM-22(H_2O_2) and the higher Al structure in MCM-22(H_2O_2). It can be assumed that the removal of the template from MCM-22(P) utilizing H_2O_2 treatment may prevent the dealumination and successfully maintain the acidic sites. In addition, from Fig. 8, it can be observed that both Zn-MCM-22(C) and Zn-MCM-22(H_2O_2) have higher acidic sites densities compared with the catalysts without Zn loading for the presence of Lewis acid center that resulted from the Zn moiety on the MCM-22. In the meantime, the acidic

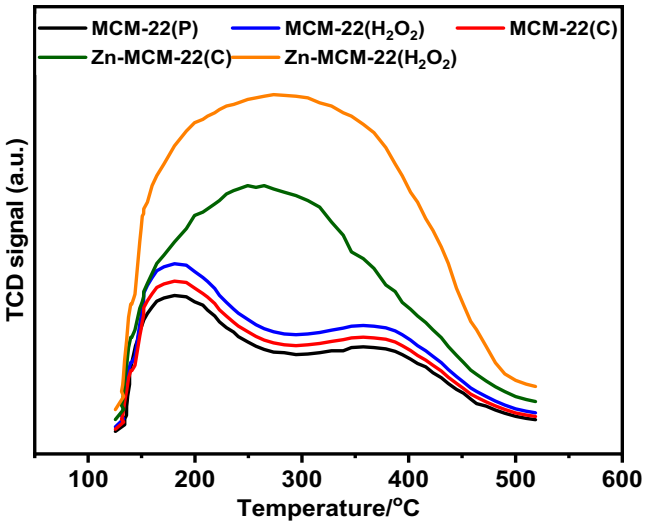

Fig. 8 The NH_3-TPD pattern profiles of the synthesized MCM-22 catalysts

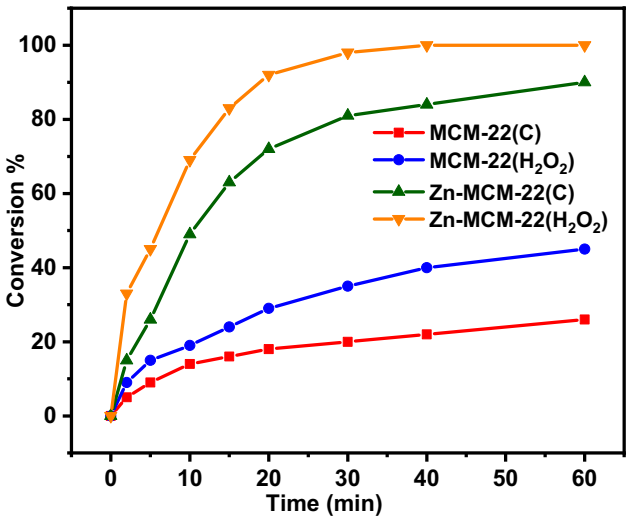

Fig. 9 The conversion percentages of benzene over the MCM-22 catalysts with and without Zn loading. The reaction conditions: 0.5 mol benzene, 0.025 mol BC, 80 °C and 25 mg cm^{-3} of catalyst

site density of the Zn-MCM-22(H_2O_2) is higher than that of the Zn-MCM-22(C) for the presence of Si–OH silanol groups bound to the MWW structure layer in the Zn-MCM-22(H_2O_2) catalyst.

3.6 The catalytic activity

The catalytic activity of the Zn-MCM-22(C) and the Zn-MCM-22(H_2O_2) catalysts synthesized by removing the HMI template from the MCM-22(P) zeolite by thermal calcination and H_2O_2 oxidation, respectively, was evaluated based on benzene alkylation by benzyl chloride through the Friedel–Crafts reaction. Figure 9 shows the conversion percentages of benzene alkylation via benzyl chloride above the MCM-22(C) and MCM-22(H_2O_2) catalysts through Friedel–Crafts reaction. It can be clearly seen that the activity of the oxidised MCM-22(H_2O_2) had a higher conversion efficiency versus the calcined MCM-22(C) catalysts. It could be inferred that calcination of MCM-22(P) causes some of the initial Si–O–Al bonds to decompose, and that H_2O_2 treatment for MCM-22(C) allows the original structure of MCM-22 to be preserved, preventing Al atoms from escaping from the zeolite framework and increasing the number of accessible acid sites as the surface area increases [29]. The role of zinc nanoparticles loaded on the detemplated zeolites on their catalytic activity in benzene alkylation through Friedel–Crafts reaction was also considered. As shown in Fig. 9 and Table 3, the Zn-MCM-22(H_2O_2) catalyst exhibits a high conversion and the alkylation reaction of benzene completed in 40 min versus a 60 min for the same reaction with the

Table 3 Alkylation results of conversion of benzene and selectivity of mono and dibenzylation over different catalysts

Catalysts	Time (min)	Conversion (%)	Monobenzylation (%)	Dibenzylation (%)
MCM-22(C)	60	26	99.0	1.0
MCM-22(H_2O_2)	60	45	98.97	1.03
Zn-MCM-22(C)	60	81.17	98.99	1.01
Zn-MCM-22 (H_2O_2)	60	100.00	95.98	4.02

Zn-MCM-22(C) catalyst. This indicates that the number of acidic sites above the Zn-MCM-22(H_2O_2) is greater than that above the Zn-MCM-22(C) due to a higher concentration of bridging hydroxyl (SiOHAl) groups and more Al structure in the MCM-22(H_2O_2). In brief, the catalytic activity of the MCM-22(H_2O_2) is greater than the MCM-22(C) since the MCM-22(H_2O_2) has more 10-ring channels, 12-ring pockets (C) and Si–OH silanol groups connected to the MWW structure layer.

Figure 10 shows a schematic sketch of a detailed mechanism of benzene alkylation by benzyl chloride. It involves the surface-active sites of the catalyst zinc chloride supported on the MCM-22. The interaction between the benzyl chloride and the zinc metal on the catalyst surface forms a weak interaction between the Cl and Zn atoms and thereof may weaken the C–Cl bond.

To further understand the activity of the presently synthesized catalysts in the conversion percentages of benzene alkylation, Table 4 compares the results obtained from relevant published studies. The Zn-MCM-22(H_2O_2) showed its premium efficiency of 100% in the alkylation of benzene in relation to the other catalysts.

Figure 11 shows the conversion percentages for the Zn-MCM-22(C) and the Zn-MCM-22(H_2O_2) catalysts after five times leaching test. Both catalysts showed their perfect stablility after five times of the reusability test without obvious change in their activities. In the meantime, Zn-MCM-22(H_2O_2) catalyst had more stability than Zn-MCM-22(C).

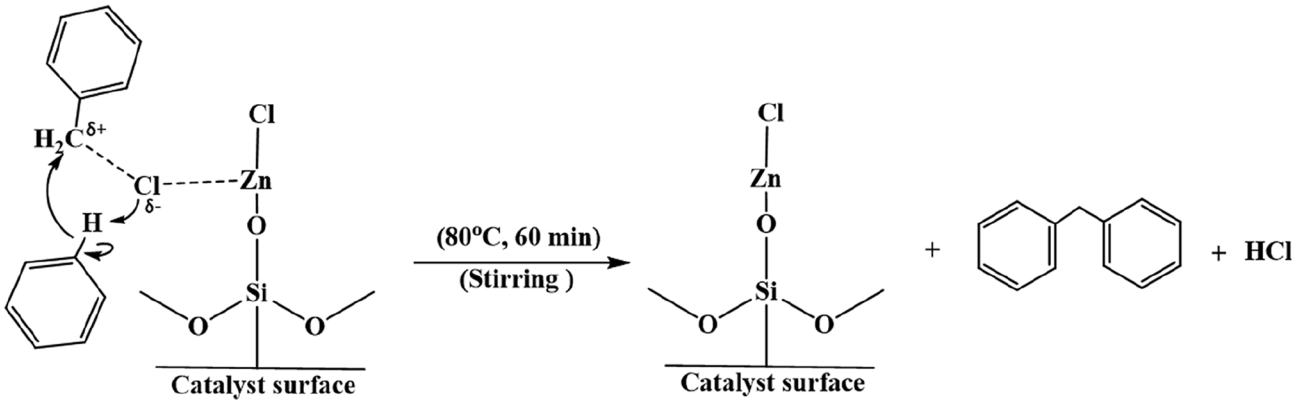

Fig. 10 Schematic sketch showing the mechanism of the Friedel-Grafts benzylation of benzene with benzyl chloride

Table 4 A comparison of the conversion efficiency for the Zn-MCM-22(H_2O_2) prepared in this study with the catalysts used in the previous studies

Samples	Conversion (%)	Si/Al ratio	Reaction conditions	Refs.
Zn-MCM-22 (H_2O_2)	100	50	0.5 mol benzene, 0.025 mol BC, Temp = 80 °C, Time = 1 h, and 25 mg cm^{-3} of the catalyst	This study
MCM-22	76.05	15	Pressure = 3.5 MPa	[30]
BEA zeolite	76.25	13	Temp = 180 °C, Time = 2 h, WHSV propane = 6.2 h^{-1}	
MIL-101-Fe	72.9	–	Temp = 150 °C, gas phase condition	[31]
MIL-88-Fe	72.1			
ZSM-5	12.2	7.86	Liquid phase alkylation of benzene. Temp = 70 °C,	[32]
Mordinate-MOR	40.0	19.60	Time = 4 h, Atmspheric pressure, and 0.5 g of catalyst	
BEA	86.6	12.92		
HY-zeolite	63.7	3.30		
Acid-treated ZSM-5	40	44.9	Atmospheric pressure	[33]
Alkali treated ZSM-5	43	29.1	0.5 g of the catalyst, fixed bed reactor, and WHSV = 2 h^{-1}	
H-beta zeolite	20	38.6	Alkylation of benzene with isobutylene, fixed bed reactor, pressure = 3.5 MPa, WHSV = 4 h^{-1}, Temp = 240 °C	[34]
BEA	23	4.8	0.5 g of the catalyst	[35]
FAU	8	6.0	Time = 1 h, Temp = 180 °C *n*-heptane as GC internal	

WHSV weight hour space velocity, MIL-101-Fe is Metal–organic frameworks (MOFs)

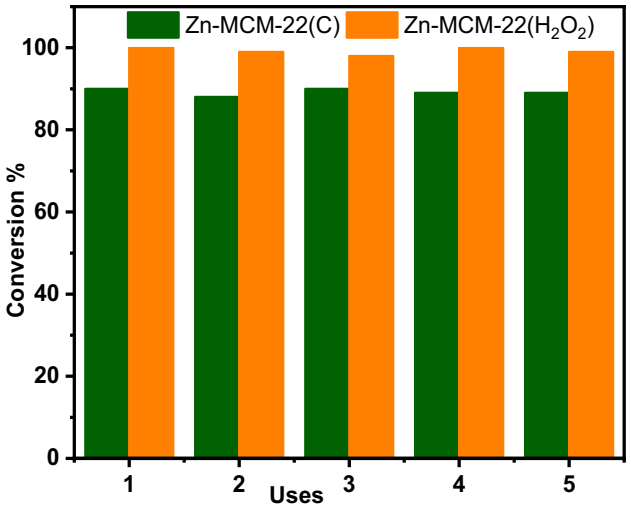

Fig. 11 Reusability of the Zn-MCM-22(C) and the Zn-MCM-22(H_2O_2) after five uses. Reaction conditions: 0.5 mol benzene, 0.025 mol BC, 80 °C and 25 mg cm^{-3} of catalyst

Table 5 MP-AES analysis of the filtered liquid

	Zn-MCM22(C)		Zn-MCM22(H_2O_2)	
	Fresh	Used	Fresh	Used
Concentration of Zn (ppm)	0.04	(0.06)[a](0.04)[b]	0.05	(0.05)[a](0.06)[b]
% of Zn resulting	0.15	(0.21)[a] (0.15)[b]	0.18	(0.18)[a](0.21)[b]

[a]1st used

[b]5th used

This is attributed again to the high concentration of (SiOHAl) groups and the more Al structure in the Zn-MCM-22(H_2O_2) catalyst.

The MP-AES examination of the filtered liquid of Zn-MCM22(C) and Zn-MCM22(H_2O_2) from each use of the recyclability study showed almost negligible concentrations of zinc particles, which have leached from the fresh catalysts as shown in Table 5.

4 Conclusions

Based on the results obtained, we can conclude that the H_2O_2 treatment was a more efficient method in the removal of the organic HMI template from the precursor MCM-22(P) than the thermal calcination. The surface area and the pore volume of the detemplated zeolite by H_2O_2 treatment increased without comprising the crystalline structure. The creation of extra frame Al decreased because of the treatment low temperature. Besides, the condensation of the silanol groups (–Si–O–H) on the exterior layer of the MCM-22 layers has restricted which induces a higher amount of the intercrystal pores.

The benzylation conversion of benzene with the aid of MCM-22(H_2O_2) was more active than that of MCM-22(C). The loading of zinc into the detemplated zeolites resulted in an enhanced catalytic performance and much higher conversions for the presence of acidic sites. Interestingly, we can reveal that the detemplation method with H_2O_2 can be ideal for some other forms of MWW zeolites whose structures and properties would be simply affected by the direct calcination with the extraction of the template.

References

1. S.L. Lawton et al., Twelve-ring pockets on the external surface of MCM-22 crystals. Microporous Mesoporous Mater. **23**(1), 109–117 (1998)
2. A. Ahmad et al., Synthesis, characterization and catalytic testing of MCM-22 derived catalysts for n-hexane cracking. Sci. Rep. **10**(1), 21786 (2020)
3. X. Ren, J. Liang, J. Wang, H-MCM-22 zeolitic catalysts modified by chemical liquid deposition for shape-selective disproportionation of toluene. J. Porous Mater. **13**(3), 353–357 (2006)
4. P. Sahu et al., Cerium ion-exchanged layered MCM-22: preparation, characterization and its application for esterification of fatty acids. J. Porous Mater. **25**(4), 999–1005 (2018)
5. Y. Shang et al., Modification of MCM-22 zeolites with silylation agents: acid properties and catalytic performance for the skeletal isomerization of n-butene. Catal. Commun. **9**(5), 907–912 (2008)
6. F.S.O. Ramos, M.K. de Pietre, H.O. Pastore, Lamellar zeolites: an oxymoron? RSC Adv. **3**(7), 2084–2111 (2013)
7. W.J. Roth, J. Čejka, Two-dimensional zeolites: dream or reality? Catal. Sci. Technol. **1**(1), 43–53 (2011)
8. U. Díaz, A. Corma, Layered zeolitic materials: an approach to designing versatile functional solids. Dalton Trans. **43**(27), 10292–10316 (2014)
9. G.G. Juttu, R.F. Lobo, Characterization and catalytic properties of MCM-56 and MCM-22 zeolites. Microporous Mesoporous Mater. **40**(1), 9–23 (2000)
10. M. Müller, G. Harvey, R. Prins, Comparison of the dealumination of zeolites beta, mordenite, ZSM-5 and ferrierite by thermal treatment, leaching with oxalic acid and treatment with SiCl4 by 1H, 29Si and 27Al MAS NMR. Microporous Mesoporous Mater. **34**(2), 135–147 (2000)
11. V. Valtchev et al., Tailored crystalline microporous materials by post-synthesis modification. Chem. Soc. Rev. **42**(1), 263–290 (2013)
12. J. Patarin, Mild methods for removing organic templates from inorganic host materials. Angew. Chem. Int. Ed. **43**(30), 3878–3880 (2004)
13. L. Lang et al., Importance of hydrogen for low-temperature detemplation of high-silica MFI zeolite crystals. Microporous Mesoporous Mater. **235**, 143–150 (2016)
14. J. He et al., New methods to remove organic templates from porous materials. Mater. Chem. Phys. **77**(1), 270–275 (2003)
15. J. Kuhn et al., Detemplation of DDR type zeolites by ozonication. Microporous Mesoporous Mater. **120**(1), 12–18 (2009)
16. H. Xing et al., Detemplation with H_2O_2 and characterization of MCM-56. Catal. Commun. **9**(2), 234–238 (2008)

17. L. Xu et al., Synthesis, characterization and catalytic performance of a novel zeolite ITQ-2-like by treating MCM-22 precursor with H_2O_2. Bull. Mater. Sci. **34**(7), 1605–1610 (2011)
18. I. Melián-Cabrera, F. Kapteijn, J.A. Moulijn, One-pot catalyst preparation: combined detemplating and Fe ion-exchange of BEA through Fenton's chemistry. Chem. Commun. **16**, 2178–2180 (2005)
19. S.V. Lande et al., Zinc-modified MCM-22 as potential solid acid catalyst for Friedel-Crafts alkylation reaction. Int. J. Chem. React. Eng. **11**(1), 407–415 (2013)
20. A. Corma, C. Corell, J. Pérez-Pariente, Synthesis and characterization of the MCM-22 zeolite. Zeolites **15**(1), 2–8 (1995)
21. A. Corma et al., Infrared spectroscopy, thermoprogrammed desorption, and nuclear magnetic resonance study of the acidity, structure, and stability of zeolite MCM-22. Zeolites **15**(7), 576–582 (1995)
22. Q.-Q. Hao et al., The delaminating and pillaring of MCM-22 for Fischer-Tropsch synthesis over cobalt. Catal. Today **274**, 109–115 (2016)
23. M. Hu et al., Effect of template removal using plasma treatment on the structure and catalytic performance of MCM-22. RSC Adv. **8**(28), 15372–15379 (2018)
24. J.K. Reddy et al., Synthesis of Ce-MCM-22 and its enhanced catalytic performance for the removal of olefins from aromatic stream. J. Porous Mater. **27**(6), 1649–1658 (2020)
25. Y. Liu et al., Facile and fast template removal from mesoporous MCM-41 molecular sieve using dielectric-barrier discharge plasma. Catal. Commun. **11**(6), 551–554 (2010)
26. A. Al-Nayili, M. Albdiry, N. Salman, Dealumination of zeolite frameworks and Lewis acid catalyst activation for transfer hydrogenation. Arab. J. Sci. Eng. **46**(6), 5709–5716 (2021)
27. J. Kuhn et al., Detemplation of [B]MFI zeolite crystals by ozonication. Microporous Mesoporous Mater. **120**(1), 35–38 (2009)
28. C.S. Triantafillidis, A.G. Vlessidis, N.P. Evmiridis, Dealuminated H−Y zeolites: influence of the degree and the type of dealumination method on the structural and acidic characteristics of H−Y zeolites. Ind. Eng. Chem. Res. **39**(2), 307–319 (2000)
29. A. Korzeniowska et al., The structure-catalytic activity relationship for the transient layered zeolite MCM-56 with MWW topology. Catal. Today **345**, 116–124 (2020)
30. A. Corma, V. Martínez-Soria, E. Schnoeveld, Alkylation of benzene with short-chain olefins over MCM-22 zeolite: catalytic behaviour and kinetic mechanism. J. Catal. **192**(1), 163–173 (2000)
31. E. Rahmani, M. Rahmani, Alkylation of benzene over Fe-based metal organic frameworks (MOFs) at low temperature condition. Microporous Mesoporous Mater. **249**, 118–127 (2017)
32. S.K. Saxena, N. Viswanadham, Aa.H. Al-Muhtaseb, Effect of zeolite pore morphology on solvent-less alkylation of benzene with 1-hexene. Mater. Today Chem. **4**, 45–52 (2017)
33. Q. Wang et al., Influence of the post-treatment of HZSM-5 zeolite on catalytic performance for alkylation of benzene with methanol. Chin. J. Chem. Eng. **25**(12), 1777–1783 (2017)
34. X. Wang et al., N-methyl-2-pyrrolidone-induced conversion of USY into hollow Beta zeolite and its application in the alkylation of benzene with isobutylene. Microporous Mesoporous Mater. **294**, 109944 (2020)
35. S.F. Rastegar et al., Analysis of decisive structural parameters of zeolites for alkylation of benzene with ethylene. Appl. Catal. A **591**, 117379 (2020)